Crystal Structural Studies of a Membrane Protein Complex, Cytochrome *c* Oxidase from Bovine Heart

Tomitake Tsukihara[a]* and Shinya Yoshikawa[b,c]

[a]*Institute for Protein Research, Osaka University, 3-2 Yamada-oka, Suita 565, Japan,* [b]*Department of Life Science, Himeji Institute of Technology, Kamigohri, Akoh, Hyogo 687-12, Japan, and* [c]*CREST, Japan Science and Technology Corporation (JST), Kamigohri, Akoh, Hyogo 687-12, Japan. E-mail: tsuki@protein.osaka-u.ac.jp*

Abstract

Membrane proteins invest the membranes of living cells and organelles with such functions as energy conversion, molecular transport and signal transduction. The number of known structures of membrane proteins is less than 20, which is too few to understand the highly organized biological reactions in a cell. The whole procedure, including crystallization, for bovine heart cytochrome *c* oxidase is described as an example of crystal structural analysis of a membrane protein. Structural features of membrane proteins and structure–function relationships of the enzyme are also discussed.

Tomitake Tsukihara graduated from the Faculty of Pharmaceutical Sciences of Osaka University and did graduate work at the Institute for Protein Research, Osaka University, under the guidance of Professor Masao Kakudo. He obtained a PhD in Chemistry in 1974 for his work on crystal structural studies of cytochrome c from bonito heart. He moved to Tottori University in 1971 and stayed there until 1991, when he became a Professor at the University of Tokushima. He took up his present position in 1995. He was a Research Associate at the Department of Biological Science at Purdue University from 1978 to 1980, where he learned crystallography of biological macromolecular assemblies from Professor Michael G. Rossmann. He has collaborated with Professor S. Yoshikawa in crystallographic research on cytochrome c for more than 20 years.

Shinya Yoshikawa did undergraduate and graduate studies at the Department of Biology of Osaka University under the guidance of Professor Kazuo Okunuki and obtained his PhD in Biochemistry in 1970. He worked at the Department of Biology, Konan University, Kobe, from 1972 to 1988, then moved to his present institution in 1988 as a Professor. He was a visiting Professor at the Department of Biochemistry, Colorado State University, where he learned the true biochemistry from Professor Winslow S. Caughey. His main research interest has been in the reaction mechanism of cytochrome c oxidase since his graduate student days.

1. Introduction

Cells, especially eukaryotic cells, contain organelles with membranous structures coated by a phospholipid bilayer. One of the roles of these membranes is to provide compartments to prevent confusion in many chemical processes in the cells. However, most biological membranes incorporate proteins termed 'membrane protein' to provide the organelles with such various functions as energy conversion, molecular transportation and signal transduction besides partitioning the cell space. Since the structure of the reaction center of *Rhodopseudomonas viridis* (Deisenhofer *et al.*, 1984, 1985) was solved as the first crystal structure of a membrane protein by X-ray crystal structure analysis at 3.0 Å resolution, almost 20 structures of membrane proteins have been obtained at higher than 3.5 Å resolution by X-ray crystal structure analysis and two-dimensional electron diffraction. Most of them are membrane protein complexes consisting of multiple subunits. The number of known structures of membrane proteins is too few to understand the highly organized biological reactions in the cell. Crystallographic studies on membrane proteins must be increased. The whole procedure of crystal structure analysis of cytochrome *c* oxidase (CcO) from bovine heart is described as an example of structural analysis of a membrane protein complex. Structural features and structure–function relationships of the enzyme are also discussed in the present paper.

Bovine heart CcO is a large multicomponent membrane protein complex consisting of 13 different polypeptide subunits, 2 hemes *a* and two Cu-atom sites as redox active centers, one Zn atom, one Mg atom (Malmström, 1990; Ferguson-Miller & Babcock, 1996) and one Na or Ca atom (Yoshikawa, Shinzawa-Itoh *et al.*, 1998). This membrane protein complex is a typical hybrid protein whose three subunits are encoded by mitochondrial DNA and the other ten subunits are encoded by nuclear DNA (Capaldi, 1990). The mol-

ecular mass of the enzyme calculated for the protein moiety is 204 005 Da. This enzyme catalyzes reduction of O_2 to H_2O coupled with proton pumping across the mitochondrial inner membrane (Malmström, 1990; Ferguson-Miller & Babcock, 1996). We have reported the structure of the oxidized enzyme at 2.8 Å resolution (Tsukihara *et al.*, 1995, 1996; Tomizaki *et al.*, 1998) and at 2.3 Å (Yoshikawa, Shinzawa-Itoh *et al.*, 1998), a fully reduced enzyme at 2.35 Å, a fully reduced CO-bound enzyme at 2.8 Å and an oxidized azide-bound enzyme at 2.9 Å (Yoshikawa, Shinzawa-Itoh *et al.*, 1998). Crystal and molecular structures of four-subunit and two-subunit bacterial CcO's have been reported at 2.8 Å (Iwata *et al.*, 1995) and 2.7 Å (Ostermeier *et al.*, 1997).

2. Crystallization

In order to crystallize a protein, first a method for obtaining a stable purified protein in large quantities has to be established. Membrane proteins themselves are unstable either in organic solvent or in aqueous solution because they have both hydrophilic and hydrophobic surfaces. Thus, any purified membrane protein should be most stable in aqueous solvent when the hydrophobic surface is covered with detergent molecules in a mixed-micelle state. Up to now, all the membrane protein crystals that diffract X-rays up to 3.5 Å resolution have been obtained from purified preparations solubilized with detergents. The establishment of a purification method is the hardest part of crystallization. Integrity in the conformation of a protein is much more important than the chemical purity of the protein. In other words, slightly denatured protein molecules strongly interfere with crystallization of the protein. Unnecessary trials for complete removal of an impurity, such as repeated applications of chromatographic separation, are likely to cause denaturations. Thus, sometimes, a purer preparation is less suitable for crystallization.

For crystallization of membrane proteins, the most important interaction between the protein molecules in the crystal lattice for stabilizing the crystals is the one between the hydrophilic surfaces, since only these interactions can be specific. The detergent molecules on the hydrophobic surface cannot be fixed specifically to membrane proteins since phospholipids in a biological membrane are replaced with the detergent on solubilization of the membrane protein. Thus, these detergents are unlikely to participate in any specific and strong interactions between the protein molecules in the crystal lattice. Based on these considerations, a strategy for crystallization of membrane proteins has been proposed (Michel, 1983; Garavito & Picot, 1990). In order to promote the interaction between the hydrophilic surfaces of adjacent protein molecules, membrane proteins should be solubilized with small-sized detergents. On the other hand, large membrane proteins could have stronger interactions if the hydrophilic surface is larger. Thus, antibody Fv fragments have been used for enlarging the hydrophilic surface. Bacterial CcO has been crystallized from an enzyme preparation treated with its monoclonal antibody Fv fragments (Ostermeier *et al.*, 1995). The crystal packing indicates that the crystals are stabilized only by the interaction between the Fv fragments attached to the enzyme. These results suggest that the role of the detergent is only to stabilize the membrane protein in aqueous solution.

However, effects of detergent structure on crystallization conditions of bovine heart CcO indicate that detergent molecules also contribute to the stability of membrane protein crystals. Bovine heart CcO is crystallized by various kinds of alkyl polyoxyethylene, sometimes very specifically. The crystallization conditions are very sensitive to the length of the polyoxyethylene chain. The enzyme preparation stabilized with Brij-35 [$CH_3(CH_2)_{11}(OCH_2CH_2)_{23}OH$] provides a hexagonal bipyramidal crystal at low ionic strength (Yoshikawa, Tera *et al.*, 1988). The detergent provides also tetragonal plate crystals at higher ionic strength (Shinzawa-Itoh *et al.*, 1995). The tetragonal plate crystals appear also from the enzyme preparation stabilized with the alkyl polyoxyethylene with shorter polyoxyethylene chain down to six oxyethylene units (Shinzawa-Itoh *et al.*, 1995). The alkyl polyoxyethylene $CH_3(CH_2)_{11}(OCH_2CH_2)_5OH$ does not give any crystal (Shinzawa-Itoh *et al.*, 1995). Only Brij-35 gives the hexagonal bipyramidal crystals. Two alkyl polyoxyethylenes, $CH_3(CH_2)_{11}(OCH_2CH_2)_8OH$ and $CH_3(CH_2)_{11}(OCH_2CH_2)_7OH$, provide tetragonal column crystals (Shinzawa-Itoh *et al.*, 1995). The highest resolutions so far obtained are 6.0 Å for hexagonal bipyramidal crystals, 5.0 Å for tetragonal column crystals and 10.0 Å for tetragonal plate crystals (Shinzawa-Itoh *et al.*, 1995). These results indicate that too small a detergent does not work in any crystallization given above, although they are effective for stabilizing the enzyme in aqueous solution. Thus, these detergents at the right sizes seem to contribute to the stabilization of the crystals. The effect of the detergent structure given above indicates that crystals with higher specificity in the detergent structure diffract X-rays up to higher resolution. The correlation also suggests that the structure of the detergent is critical for stabilizing crystals and thus for improving the quality of crystals.

Critical micellar concentration (CMC) of alkyl-polyoxyethylene is mainly determined by the size of the alkyl chain. However, crystallization conditions are hardly affected by the structure of the alkyl chain. That is, crystallization conditions of the preparations stabilized with alkyl polyoxyethylenes with $CH_3(CH_2)_9$ as the alkyl moieties were strictly identical to those for the preparation stabilized with $CH_3(CH_2)_{11}$ polyoxyethylenes, except for the requirement of higher concentration of the detergent in the medium for adjusting

the one order-of-magnitude-higher CMC of $CH_3(CH_2)_9$ polyoxyethylenes.

The specificity of an alkyl sugar-type detergent to crystallization conditions is much higher than that of alkyl polyoxyethylene-type detergent. The CcO preparation stabilized with decylmaltoside forms orthorhombic crystals that diffract X-rays up to 2.8 Å resolution (Tsukihara *et al.*, 1995). Among all the commercially available alkyl and fatty acyl sugar-type detergents, only this detergent provides the ortho-rhombic crystals. Not only the sugar moiety but also the size of the alkyl chain are critical. Neither dodecyl maltoside nor octyl maltoside provides orthorhombic crystals though both detergents are effective for stabi-lizing the enzyme in an aqueous medium.

This extremely high structural specificity of detergent for crystallization indicates that at least some of the detergent molecules are bound specifically and thus tightly to the hydrophobic surface to place the protein molecules specifically in the crystal lattice.

As given above, the detergent species greatly influ-ences crystallization conditions. Exchanging detergent species often corresponds to exchanging protein species in crystallization. This is a great advantage of membrane protein crystallization against crystallization of water-soluble proteins. In other words, any membrane protein could be crystallized once purified and stabilized in aqueous solution with the right detergent. For judging whether a detergent is the right one for the crystal-lization, the specificity of the detergent species could be useful.

Of course, many factors other than detergent species are critical for crystallization. In the case of bovine heart CcO, solubilization of the enzyme from mitochondrial membrane with ultra-pure cholic acid and complete removal of slightly denatured enzyme with recrystalliz-ation have improved the resolution of X-ray diffraction from 2.8 to 2.3 Å (Yoshikawa, Shinzawa-Itoh *et al.*, 1998). Even some diffraction spots were observed up to 1.9 Å resolution. As stated above, decylmaltoside is the best detergent for crystallization of bovine heart CcO so far. We are now searching for a better detergent by modifying the structure of decylmaltoside.

3. Crystal structure determination

3.1. *Intensity data collection*

Crystals of membrane proteins deteriorate more easily than those of water-soluble proteins. The ortho-rhombic crystal of oxidized CcO from bovine heart crystallized by equilibration with 0.6% polyethylene glycol (PEG) solution was soaked in a 5% PEG solution to stabilize the crystal. Although X-ray diffraction experiments of the present report are undertaken at 280 to 283 K, the crystals have been successfully frozen at around 100 K by equilibration with 30 to 35% glycerol solution for future higher-resolution analysis. A crystal of chicken heart cytochrome bc_1 complex, a membrane protein complex, was successfully frozen using glycerol as a cryoprotectant (Zhang *et al.*, 1998). These experi-ments imply that crystals of membrane protein complexes can be frozen by choosing an appropriate cryoprotectant as is the case for water-soluble proteins.

The orthorhombic CcO crystal belongs to space group $P2_12_12_1$ with unit-cell dimensions $a = 189.1\,(1)$, $b = 210.5\,(1)$ and $c = 178.6\,(1)$ Å. Intensity data for the native crystals and heavy-atom derivatives were collected on the BL6A2 station at the Photon Factory (PF) by the oscillation method using a Weissenberg
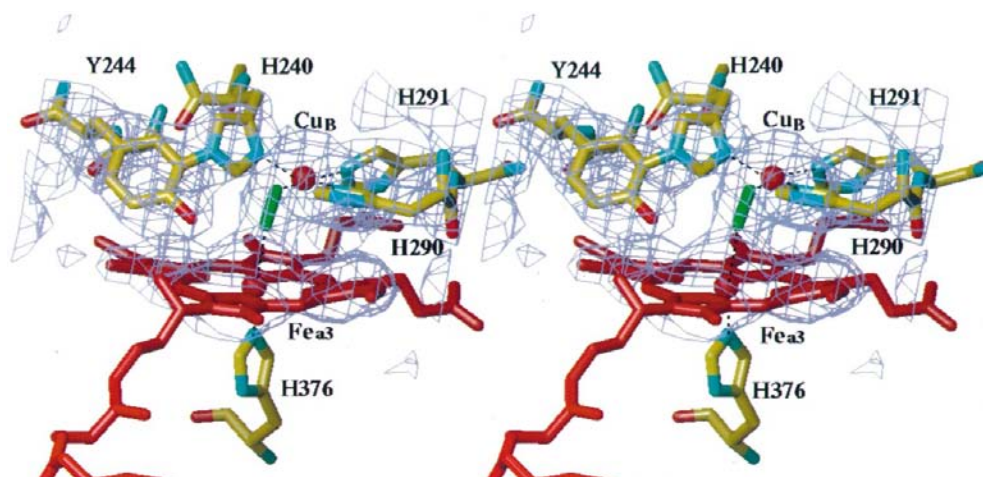

Fig. 1. Stereoscopic drawing of MIR/DM electron-density map of the dioxygen reduction site of oxidized CcO from bovine heart at 2.3 Å resolution. Cages are drawn at the 1σ level ($1\sigma = 0.16$ e Å^{-3}). The refined structure around the active site is superposed well on the map. His240 and Tyr244 are linked together by a covalent bond between Nε2 of the imidazole group and Cε2 of the phenol group, a peroxide group drawn in green bridges Fe$_{a_3}$ and Cu$_B$.

camera designed by Sakabe (1983) for macromolecules equipped with an imaging plate (Fuji Film Co. Ltd). The cylindrical cassettes with radii 540 or 870 mm were filled with helium gas to increase the signal-to-noise ratio. X-rays of wavelength 1.00 Å were focused with a double mirror and a 0.1 mm diameter collimator. The Weissenberg camera with a large cassette has been proved to be an excellent system to collect intensity data for macromolecular crystals with a large unit cell (Jones *et al.*, 1993; Jacobson *et al.*, 1994). This system was used for intensity data collection of bacterial four-subunit CcO (Iwata *et al.*, 1995).

Each oscillation image was taken with exposure time of 40 to 100 s for 2.8 Å data collection and 300 to 360 s for 2.3 Å data collection without any alignment of the rotation axis. The oscillation range of each image was 1.0° for 2.8 Å and 0.5° for 2.3 Å without any overlap between adjacent images. A fresh position was used for every 1000 to 2000 s of exposure time and three to five positions of a crystal were shot by X-rays.

Each oscillation frame was processed by *DENZO* (Otwinowski, 1993). Scale factor, crystal setting parameters and mosaicity of each frame were refined by *SCALEPACK* (Otwinowski, 1993). Local scaling was applied to provide an absorption correction in order to detect Bijvoet differences due to Zn, Cu and Fe atoms in the native crystal (Tsukihara *et al.*, 1995). Estimated mosaicities of oxidized CcO crystals are as low as about 0.05° at the initial stage of X-ray exposure. Assuming divergency of the X-ray beam at the PF is 0.02°, the mosaicity of the crystal itself is around 0.03° before the X-ray irradiation, which is nearly equal to that of crystals of water-soluble proteins. The mosaicity and overall temperature factor increased gradually with X-ray exposure time. Each frame with a mosaicity less than 0.20° and a relative temperature factor lower than 10 Å^2 *versus* the standard frame was used to generate intensity data sets with high quality. 973 307 observed reflections of the oxidized crystal from 211 frames were merged into 284 634 independent reflections with a completeness of 90.2% and an R_{merge} of 6.1% at 2.3 Å resolution. The observations-to-parameters ratio is about 2.0, which is about 1.5 times that of ordinary protein crystals diffracting to the same resolution. This is because of a high solvent content of 72% in volume in comparison with the ordinary crystals with 50% solvent content. Solvent contents of most membrane proteins are as high as 70% as follows: *Rhodopseudomonas viridis* photosynthetic reaction center 77% (Deisenhofer *et al.*, 1984); *Escherichia coli* porin 58% (Cowan *et al.*, 1992); prostaglandin H2 synthase-1 72% (Picot *et al.*, 1994); photosynthetic bacterial light-harvesting complex II 72% (McDermott *et al.*, 1995); bovine heart CcO 72% (Tsukihara *et al.*, 1995); staphylococcal α-hemolysin 59% (Song *et al.*, 1996); photosynthetic purple bacterial light-harvesting complex II 71% (Koepke *et al.*, 1996); cyanobacterium photosystem I 80% (Krauss *et al.*, 1996);

Paracoccus denitrificans two-subunit CcO 72% (Ostermeier *et al.*, 1997); bovine heart cytochrome bc_1 complex 65% (Xia *et al.*, 1997). Thus, for a given diffraction limit, an observations-to-parameters ratio of a membrane protein is far higher than that of an ordinary protein crystal, which is an advantage for the crystal structure analysis of membrane proteins.

3.2. *Phase determination by multiple isomorphous replacement and phase refinement by density modification*

The determination of heavy-atom sites of each derivative is initiated by solving a difference Patterson function. Crystals of membrane protein complexes have large cell dimensions proportional to their molecular weights. In general, the more heavy-atom sites there are in a unit cell of a derivative crystal, the more difficult it is to solve the difference Patterson function because of overlapping of interatomic vectors. However, eight and three heavy-atom positions in an asymmetric unit of the oxidized CcO crystal were successfully determined in difference Patterson maps for the CH_3HgCl derivative and the $IrCl_6$ (I) derivative, respectively. Although the CH_3HgCl derivative contains as many as 32 main sites in the unit cell, most of the interatomic vectors between the main sites are clearly located as separate peaks in the difference Patterson map at 5 Å resolution as shown in Fig. 3(*a*) of our previous paper (Tomizaki *et al.*, 1998). This is partly because of the larger unit-cell dimensions of the crystal compared with those of other protein crystals.

Initial phases of the oxidized CcO were determined at 3.0 Å resolution by the multiple isomorphous replacement (MIR) method (Green *et al.*, 1954) with three derivatives, of $IrCl_6$ (I), $IrCl_6$ (II) and CH_3HgCl (Yoshikawa, Shinzawa-Itoh *et al.*, 1998). The program *MLPHARE* (Otwinowski, 1991) was applied for MIR phase determination. The criteria of the MIR phasing, figure of merit of 0.36, R_{Cullis} of 0.85 for $IrCl_6$ (I), 0.87 for $IrCl_6$ (II) and 0.90 for CH_3HgCl, and phasing powers of 0.85 for $IrCl_6$ (I), 0.85 for $IrCl_6$ (II) and 0.74 for CH_3HgCl, do not indicate high quality of the phasing. The MIR phases were refined and extended to 2.3 Å resolution in 200 small steps by the density-modification (DM) method consisting of solvent flattening (Wang, 1985), histogram matching (Zhang & Main, 1990) and noncrystallographic symmetry (NCS) averaging (Bricogne, 1974, 1976). The calculated phases obtained by DM were combined with the initial phases determined by the MIR method. Program *DM* of CCP4 (Collaborative Computational Project, Number 4, 1994) was used for the phase extension. Although the quality of initial phases was not high as stated before, the phase refinement converged well to a free *R* factor (Brunger, 1992) for 5% of the reflections in each shell and a

correlation coefficient between electron densities of two independent molecules,

$$\sum(\rho_1 - \langle\rho_1\rangle)(\rho_2 - \langle\rho_2\rangle)\big/\sum[(\rho_1 - \langle\rho_1\rangle)^2(\rho_2 - \langle\rho_2\rangle)^2]^{1/2},$$

converged to 0.279 and 0.907, respectively, indicating the high quality of phases obtained. The electron-density map (MIR/DM map) obtained by the MIR method followed by DM at 2.3 Å resolution was so clear that a post-transcriptionally modified covalent bond between the side chains of His240 and Tyr244 was identified in the map as shown in Fig. 1 (Yoshikawa, Shinzawa-Itoh *et al.*, 1998). This cross-linking has been confirmed by structural refinement with the program *X-PLOR* (Brunger *et al.*, 1987) and difference Fourier calculations. Out of 3600 protein residues, 3550 residues were uniquely located in the MIR/DM map.

The efficiency of each procedure of DM was inspected in terms of the real-space correlation coefficient (Brändén & Jones, 1990) between the refined electron density and the ideal electron density. The solvent flattening followed by NCS averaging in the 2.8 Å analysis of the oxidized enzyme improved the averaged real-space correlation for side-chain atoms from 0.39 to 0.83 (Tomizaki *et al.*, 1998). An additional procedure of the histogram matching slightly improved it to 0.85. The prominent improvement provided by the solvent flattening is because of high solvent content of the membrane protein crystal. Therefore, this technique has been applied in general for the crystal structural analysis of membrane proteins since Wang's (1985) proposal.

3.3. *Structural refinement*

The crystal structure of the oxidized CcO from bovine heart was refined by *X-PLOR* (Brunger *et al.*, 1987) under structural and NCS restraints. The polypeptide stereochemical restraints used were those of Engh & Huber (1991). At the final stage of the refinement, the atomic positions of metals and their ligand atoms were inspected in the difference Fourier map calculated with coefficients of $(F_o - F_c)\exp(i\alpha_c)$, where F_o and F_c are observed and calculated structure amplitudes, respectively, and α_c is a phase angle of the calculated structure factor. A conventional R factor and a free R factor calculated for 5% of the reflections excluded from the refinement were reduced to final values of 0.190 and 0.250 at 2.3 Å resolution, respectively. The root-mean-square deviation from the standard values of bond lengths and angles of the refined structure of the oxidized enzyme are 0.012 Å and 1.73°, respectively. The mean absolute error in atomic position estimated by Luzzati plots (Luzzati, 1952) is around 0.2 Å. The main chains of the enzyme have a quite reasonable structure as shown by the Ramachandran plots (Ramakrishnan & Ramachandran, 1965) given in Fig. 2. Out of 3310 non-glycine residues, 89.8% are in the most favored regions, 9.7% in the additional allowed regions and the remaining 0.5% are in generously allowed regions.

4. Structural features

4.1. *High propensity of helix in transmembrane structures*

Wallin *et al.* (1997) analyzed the structure of bovine heart CcO in terms of secondary structure, hydrophobicity, amino-acid species and phospholipids along the molecular axis perpendicular to the membrane plane. The central ±12 Å region from the center of the transmembrane part is almost 100% α-helix and the extremely hydrophobic region extends 10 Å on either side of the center of the membrane. Two photosynthetic reaction centers (Deisenhofer *et al.*, 1984; Allen *et al.*, 1987), a bacterial CcO (Iwata *et al.*, 1995), two light-harvesting antenna complexes (McDermott *et al.*, 1995; Koepke *et al.*, 1996), two cytochrome bc_1 complexes (Xia *et al.*, 1997; Zhang *et al.*, 1998), a plant light-harvesting complex (Kuhlbrandt *et al.*, 1994) and a bacteriorhodopsin (Grigorieff *et al.*, 1996; Pebay-Peyroula *et al.*, 1997; Kimura *et al.*, 1997) fold in the α-helical conformation in the transmembrane region. Some of these structures as well as that of bovine CcO are shown in Figs. 3(*a*), (*b*) and (*c*) with Cα drawings. Although a glycine residue is a typical α-helix-breaking amino acid in the case of water-soluble proteins, glycine residues amounting to 7.1% in the transmembrane α-helices of the bovine CcO, in contrast with a low content of 0.9% in the extramembrane α-helices of the enzyme, do not break transmembrane α-helices. Since the amide group of a transmembrane α-helix is included in intrahelical hydrogen bonds and excluded from interaction with the hydrophobic surroundings, an α-helical structure consisting of hydrophobic residues, including glycine and proline residues, is more stable than irregular structures whose amide groups are exposed to the hydrophobic surroundings in the membrane. Proline residues in the transmembrane region do not break helical structures but induce kinks in the helices.

4.2. *Positive-inside rule and structure organization of a hybrid membrane protein complex*

Distributions of charged residues at both sides of the membrane are schematically shown in Fig. 4(*a*) for bovine CcO and Fig. 4(*b*) for a photoreaction center of *R. viridis*. The mitochondrially encoded core subunits of CcO are more negatively charged in the intermembrane space (outside) than in the matrix space (inside). The similar asymmetric charge distribution has been observed in the photo reaction center of *R. viridis* (Deisenhofer & Michel, 1989) and has been called the 'positive-inside' rule by von Heijne (1986). This asymmetric charge distribution across the membrane is energetically favorable considering the electric field across the membrane to be more negative on the inside.

The nuclear-coded subunits of bovine CcO do not follow the rule predicted by Gavelo & von Heijne (1992), suggesting that structural organization of the nuclear-coded subunits is determined by different factors than that of the mitochondrially encoded subunits.

Bovine CcO is a typical hybrid protein complex like other mitochondrial respiratory enzyme complexes. 3 of 13 different subunits are encoded by the mitochondrial DNA and synthesized in the matrix space of mitochondrion and the other 10 subunits encoded by the nuclear DNA are synthesized in the cytosolic space of the cell. A hierarchy of structural organization of the bovine CcO has been deduced from intersubunit interactions among 13 subunits (Tomizaki et al., 1998). The mitochondrially encoded subunits synthesized in the matrix space are inserted into the inner membrane and the nuclear-coded subunits are synthesized in the cytosolic space. The mitochondrial subunits assemble themselves into a core structure and each nuclear subunit is transported into the proper space in the mitochondrion. The nuclear subunits IV, Vb, VIa, VIb, VIc, VIIa, VIIc and VIII find their own location on the surface of the mitochondrial core structure. The subunits Va and VIIb assemble into a complex consisting of 11 subunits. A dimeric structure of the enzyme complex is formed by intermonomer interactions among the subunits I, Vb, VIa and VIb. Symbiotic evolution, a hypothesis of an evolutionary pathway for the origin of mitochondria, is reflected in the hierarchy of structural organization of the enzyme complex.

5. Reaction mechanism of CcO

CcO catalyses dioxygen reduction coupled with proton pumping. Many spectroscopic investigations of the function of the enzyme have been performed (Ferguson-Miller & Babcock, 1996) since discovery of this enzyme (Warburg, 1924). However, understanding of the reaction mechanism has been seriously limited because of lack of crystal structure of the enzyme at high resolution. Here, possible aspects of the reaction mechanism of this enzyme deduced from the crystal structures are given.

5.1. Mechanism of the dioxygen reduction

Long before the crystal structure appeared, a copper ion (Cu_B) had been discovered near the dioxygen binding heme (heme a_3) (Caughey et al., 1976). As is well known, one-electron reduction of dioxygen is energetically unfavorable but two-electron reduction is extremely favorable (Caughey et al., 1976). Thus, it has been widely accepted that Cu_B could serve as the second electron donor to the dioxygen bound at heme a_3, forming a peroxide bridging between the heme a_3 Fe and Cu_B, as an intermediate species (Caughey et al., 1976). Formation of the peroxide species is rate limited by the electron transfer from one of the metal ions over a very

short distance, 2–3 Å. Thus, the dioxygen bound form must be too unstable to detect. However, resonance Raman investigation of the intermediate species of the CcO reaction has revealed the dioxygen bound at heme a_3 in essentially the same way as in the oxygenated forms of hemoglobins and myoglobins (Han et al., 1990; Ogura et al., 1991; Varotosis et al., 1993). Another unexpected finding is that the intermediate species detectable next to the oxygenated form is a ferryloxo form (Fe=O), not the peroxo form (Kitagawa & Ogura, 1997). These results have made the role of Cu_B less clear in the dioxygen reduction mechanism. Thus, the crystal structure at high resolution was absolutely desirable.

The crystal structure at 2.3 Å resolution shows clearly a covalent linkage between Tyr244 and His240 as shown in Fig. 1 (Yoshikawa, Shinzawa-Itoh et al., 1998). The latter amino acid coordinates to Cu_B. The covalent linkage may decrease significantly the pK of Tyr244. The linkage fixes the OH group capable of forming a hydrogen bond with a dioxygen bound at heme a_3. The tyrosine OH is connected with the matrix space by a hydrogen-bond network, that is, the tyrosine can take up protons from the matrix space (Tsukihara et al., 1996). Furthermore, another heme a, located near heme a_3, is likely to be an effective electron donor to the dioxygen reduction site (Tsukihara et al., 1995). All these crystal structures suggest that a dioxygen bound at $Fe_{a_3}^{2+}$, when hydrogen bonded to Tyr244, is reduced to hydroperoxo form ($Fe_{a_3}^{2+}OOH$). The two-electron reduction process is triggered by the electron transfer from heme a to the bound dioxygen, followed by the proton transfer from Tyr244 (Tsukihara et al., 1996). The electron transfer
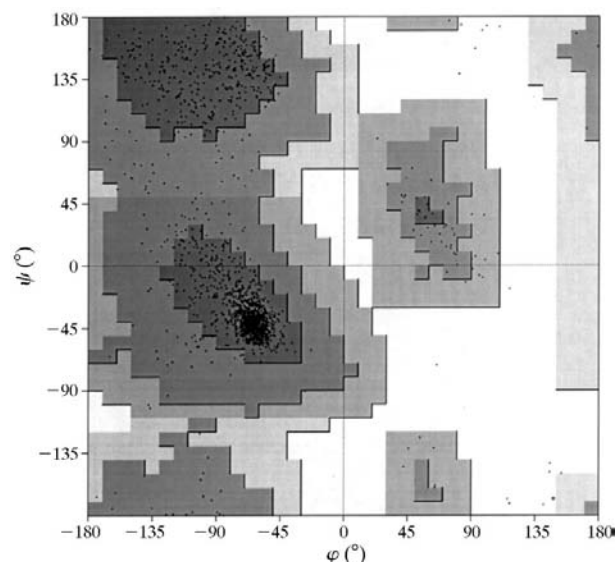

Fig. 2. Ramachandran plots (Ramakrishnan & Ramachandran, 1965) for 3560 amino-acid residues. Out of 3058 nonglycine residues, 89.9% are in the most favored regions, 9.7% in additional allowed regions and 0.5% in generously allowed regions. No residue is in disallowed regions.

from heme a to the dioxygen reduction site should be much slower than the electron transfer from Cu_B to the dioxygen bridging between Cu_B and Fe_{a_3} as has been suggested (Caughey *et al.*, 1976). The hydroperoxo bound at $Fe_{a_3}^{3+}$ is reduced to a ferryloxo form ($Fe^{4+}\!\!=\!\!\!=\!\!O$) very quickly since protons and electrons are available from Tyr244 and from Cu_B and Fe_{a_3}, respectively. Then, degradation of the oxygenated form ($Fe^{2+}O_2$) may not be so rapid while the hydroperoxo form should be very

unstable. These kinetic properties predicted from the crystal structures are fully consistent with the resonance Raman results given above (Kitagawa & Ogura, 1997).

The bridging peroxide between Cu_B and Fe_{a_3} (Fig. 1) discovered in the resting oxidized form at 2.3 Å resolution is one of the unexpected structures (Yoshikawa, Shinzawa-Itoh *et al.*, 1998). Bovine heart CcO as prepared is in the resting oxidized state, which is different from the fully oxidized state involved in the
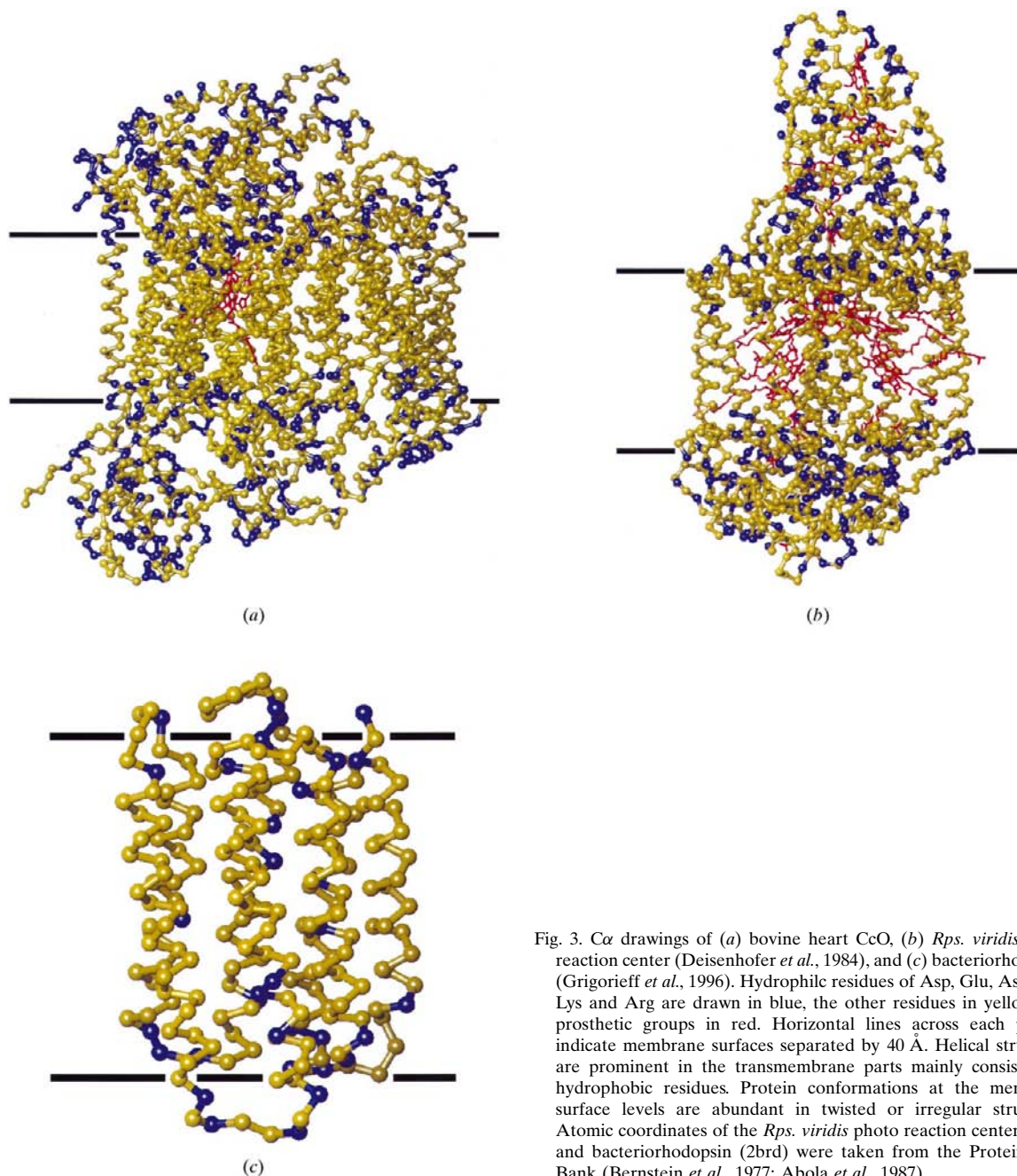

Fig. 3. Cα drawings of (*a*) bovine heart CcO, (*b*) *Rps. viridis* photo reaction center (Deisenhofer *et al.*, 1984), and (*c*) bacteriorhodopsin (Grigorieff *et al.*, 1996). Hydrophilc residues of Asp, Glu, Asn, Gln, Lys and Arg are drawn in blue, the other residues in yellow, and prosthetic groups in red. Horizontal lines across each protein indicate membrane surfaces separated by 40 Å. Helical structures are prominent in the transmembrane parts mainly consisting of hydrophobic residues. Protein conformations at the membrane surface levels are abundant in twisted or irregular structures. Atomic coordinates of the *Rps. viridis* photo reaction center (1prc) and bacteriorhodopsin (2brd) were taken from the Protein Data Bank (Bernstein *et al.*, 1977; Abola *et al.*, 1987).

catalytic turnover, in terms of the reactivity to cyanide and the electron transfer rate to heme a_3. The stability of the structure is consistent with the oxygenated form of hemerythrin in which a stable peroxide structure has been identified crystallographically (Holmes *et al.*, 1991). The slow reactivity of the resting form to cyanide (Baker *et al.*, 1987) is also consistent with the peroxide bound form.

5.2. *Mechanism of proton pumping*

Protons are transferred through a hydrogen-bond network inside the protein molecule. The crystal structure of bovine heart CcO contains many spaces inside the protein where no significant electron-density peak is detectable. Some of the spaces are large enough for placing water molecules. These spaces are likely to hold randomly oriented or mobile waters (Tsukihara *et al.*, 1996). Thus, they could serve as proton-transfer paths. Some amino-acid side chains that could form hydrogen bonds are placed near other amino acids but too far to form hydrogen bonds with them. Some of these amino-acid pairs have spaces that allow small conformational changes of the side chains without movement of main chains to form new hydrogen bonds. We call these structures possible hydrogen-bond structures (Tsuki-

Fig. 4. Schematic drawings of the transmembrane helices and asymmetric charge distributions of the extramembrane parts for (*a*) M and L subunits of *Rps. viridis* photo reaction center (Michel & Deisenhofer, 1987) and (*b*) subunits I, II and III of bovine heart CcO. The upper and lower parts of the membrane correspond to the outside and the inside, respectively. Letters N and C represent an amino terminus and a carboxyl terminus, respectively. Figures are net charges of connecting segments between two transmembrane helices. Since proton concentration inside is lower than that outside, the asymmetric charge distribution is more positive inside and stabilizes the foldings of these membrane proteins across the membranes.

hara *et al.*, 1996). Such conformational changes would be induced by changes in oxidation state and ligand-binding state of the metal sites. Population of the hydrogen-bonded state would be too low to detect in the crystal structure. The crystal structure of bovine heart CcO in the fully oxidized state involves three networks, each composed of hydrogen bonds, cavities and possible hydrogen-bond structures (Tsukihara *et al.*, 1996). One of the networks connects Tyr244 with the matrix space. Each of the other two networks connects the matrix space with the cytosolic side. However, both networks contain possible hydrogen-bond structure to prevent leaks of protons.

Recent developments in crystallographic analysis have revealed that conformations of these networks are not significantly influenced by changes in oxidation and ligand-binding states. However, a large redox-coupled conformational change occurs in a segment from Gly50 to Asp55 in subunit I as shown in Fig. 3 of a previous paper (Yoshikawa, Shinzawa-Itoh *et al.*, 1998). Asp51 among the amino acids in the segment changes the accessibility to the bulk water phase on the cytosolic side depending on the oxidation state of the metal sites (Yoshikawa, Shinzawa-Itoh *et al.*, 1998). In the fully oxidized state, the amino-acid side chain is completely buried inside the protein while it contributes to the molecular surface on the cytosolic side in the fully reduced state. This movement of the amino-acid side chain on reduction is likely to be accompanied by a significant decrease in pK of the carboxyl group, since the conformational change involves a large increase in the dielectric constant of the micro environment of the carboxyl group. Furthermore, the carboxyl group is connected with the matrix side in the oxidized state by a hydrogen-bond network, including a peptide bond, hydrogen bonds and a large cavity with a water channel from the matrix space. The carboxyl group of Asp51 is hydrogen bonded to the amide group of a peptide bond in the fully oxidized state. The carboxyl group of the peptide bond is hydrogen-bonded to Tyr54 which is connected to Arg38 located on the wall of the cavity. Thus, once the peptide amide is deprotonated by Asp51, the proton will be readily refilled by the hydrogen-bond network connecting the peptide carbonyl with the cavity. It should be noted that the peptide bond promotes the unidirectional proton transfer from Tyr54 to Asp51 since $-NH-CO-$ is much more stable than $-N=C(OH)-$ (Yoshikawa, Shinzawa-Itoh *et al.*, 1998). Furthermore, this hydrogen-bond network does not involve any possible hydrogen-bond structure. Only the peptide bond serves to stop the proton leak from the cytosolic side to the matrix side. As shown in Fig. 5, this hydrogen-bond network interacts with heme *a* with hydrogen bonds at several points, suggesting that oxidation of heme *a* promotes the proton transfer through the network towards the cytosolic space. This network does not include the dioxygen reduction site. On the other
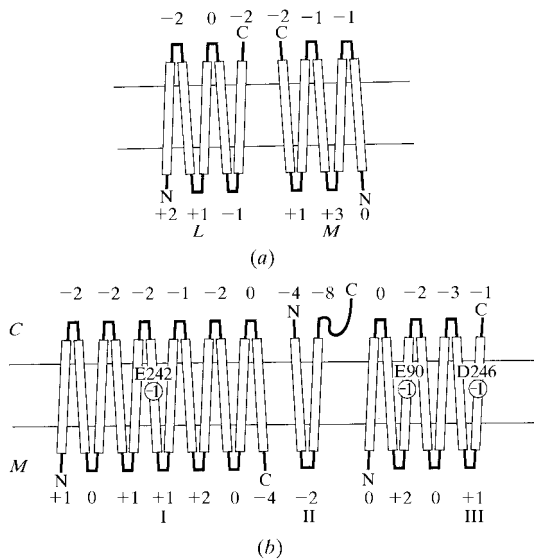
hand, one of the networks connects the matrix space with the dioxygen reduction site. Thus, the crystal structure indicates that the dioxygen reduction site is different from the proton pumping site. This mechanism is inconsistent with a proposal, the histidine cycle mechanism, in which one of the histidine imidazoles bound to Cu_B is the site for pumping protons (Wikström et al., 1994). The proposal is mainly based on comparison of the amino-acid sequences of the terminal oxidases from various organisms. That is, all the terminal oxidases reduce dioxygen to water coupled with proton pumping. On the other hand, only the amino acids coordinated to hemes a and a_3 and Cu_B are conserved among these terminal oxidases. Thus, it has been proposed that one of these amino acids has to be the site for pumping protons. Lack of one of the imidazoles bound to Cu_B in the azide-bound form of a bacterial CcO (Iwata et al., 1995) is consistent with the histidine cycle. However, all three histidines are clearly seen in the electron-density map of the azide-bound form of bovine heart CcO (Yoshikawa, Shinzawa-Itoh et al., 1998). Furthermore, Asp51 is conserved only in the animal kingdom but not in the plant and bacterial kingdoms. These facts suggests that the proton-pumping pathway of bovine heart CcO is different from those of plant and bacterial CcO. Any mechanism involving the proton-pumping site near the dioxygen reduction site, such as the histidine cycle mechanism, must have a very effective structure for sorting pumping protons from protons for making water. Without such a structure, pumping protons will be consumed for making water (Wikström et al., 1994; Williams, 1995). No such structure has been found in either bovine heart or bacterial CcO's.
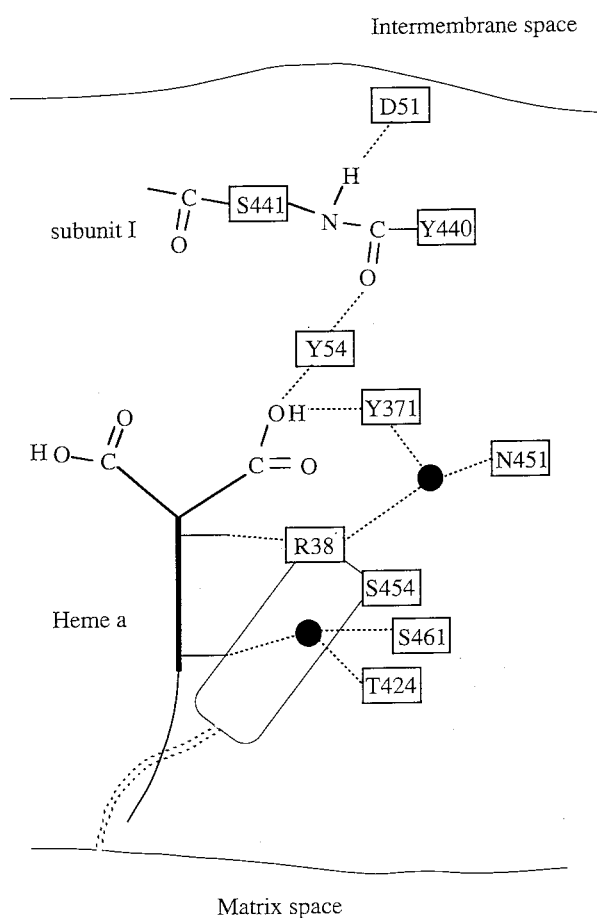
Fig. 5. The hydrogen-bond network from Asp51 of subunit I to the matrix surface. Dotted lines indicate hydrogen bonds. Closed circles are water atoms, amino acids are given by single letters with a residue number. The heme is depicted by a heavy line with two carboxyl groups, two hydroxyl groups drawn by thin short lines and a farnesylethyl group shown by a long thin line. The box near the heme is a cavity containing a water molecule with hydrogen bonds to a serine and a threonine side chains. The cavity connects to the matrix space through a channel depicted by a broken column.

References

Abola, F. C., Bernstein, F. C., Bryant, S. H., Koetzle, T. F. & Weng, J. (1987). Crystallographic Databases, pp. 107–132. Bonn/Cambridge/Chester: IUCr.

Allen, J. P., Feher, G., Yeates, T., Komiya, H. & Rees, D. C. (1987). Proc. Natl Acad. Sci. USA, **84**, 6162–6166.

Baker, G. M., Noguchi, M. & Palmer, G. (1987). J. Biol. Chem. **262**, 595–604.

Bernstein, F. C., Koetzle, T. F., Williams, G. J. B., Meyer, E. F. Jr, Bricem, M. D., Ridgers, J. R., Kennard, O., Shimanouchi, T. & Tasumi, M. (1977). J. Mol. Biol. **112**, 535–542.

Brändén, C. & Jones, A. (1990). Nature (London), **343**, 687–689.

Bricogne, G. (1974). Acta Cryst. A**30**, 395–405.

Bricogne, G. (1976). Acta Cryst. A**32**, 832–847.

Brunger, A. T. (1992). Nature (London), **355**, 472–475.

Brunger, A., Kuriyan, J. & Karplus, M. (1987). Science, **235**, 458–460.

Capaldi, R. A. (1990). Annu. Rev. Biochem. **59**, 569–596.

Caughey, W. S., Wallace, W. J., Volpe, J. A. & Yoshikawa, S. (1976). The Enzymes, 3rd ed., edited by P. D. Boyer, Vol. 13, pp. 293–344. New York: Academic Press.

Collaborative Computational Project, Number 4 (1994). *Acta Cryst.* D**50**, 760–763.

Cowan, S. W., Schirmer, T., Rummel, G., Steiert, M., Ghosh, R., Pauptit, R. A., Jansonius, J. N. & Rosenbusch, J. P. (1992). *Nature (London)*, **358**, 727–733.

Deisenhofer, J., Epp, O., Miki, K., Huber, R. & Michel, H. (1984). *J. Mol. Biol.* **180**, 385–398.

Deisenhofer, J., Epp, O., Miki, K., Huber, R. & Michel, H. (1985) *Nature (London)*, **318**, 618–624.

Deisenhofer, J. & Michel, H. (1989). *EMBO J.* **8**, 2149–2170.

Engh, R. A. Huber, R. (1991). *Acta Cryst.* A**47**, 392–400.

Ferguson-Miller, S. & Babcock, G. T. (1996). *Chem. Rev.* **96**, 2889–2907.

Garavito, R. M. & Picot, D. (1990). *Methods*, **1**, 57–69.

Gavelo, Y. & von Heijne, G. (1992). *Eur. J. Biochem.* **205**, 1207–1215.

Green, D. W., Ingram, V. M. & Perutz, M. F. (1954). *Proc. R. Soc. London Ser. A*, **225**, 287–307.

Grigorieff, N., Ceska, T. A., Downing, K. H., Baldwin, J. M. & Henderson, R. (1996). *J. Mol. Biol.* **259**, 393–421.

Han, S., Ching, Y.-C. & Rousseau, D. L. (1990). *Biochemistry*, **29**, 1380–1384.

Heijne, G. von (1986). *EMBO J.* **5**, 3021–3027.

Holmes, M. A., Le Trong, I., Turley, S., Sieker, L. C. & Stenkamp, R. E. (1991). *J. Mol. Biol.* **218**, 583–593.

Iwata, S., Ostermeier, C., Ludwig, B. & Michel, H. (1995). *Nature (London)*, **376**, 660–609.

Jacobson, R. H., Zhang, X.-J., Dubose, R. F. & Matthews, B. W. (1994). *Nature (London)*, **369**, 761–766.

Jones, E. Y., Stuart, D. I., Garman, E. F., Griest, R., Phillips, D. C., Taylor, G. L., Matsumoto, O., Darby, G., Larder, B., Lowe, D., Powell, K., Purifoy, D., Ross, C. K., Somers, D., Tisdale, M. & Stammers, D. K. (1993). *J. Cryst. Growth*, **126**, 261–269.

Kimura, Y., Vassylyev, D. G., Miyazawa, A., Kidera, A., Matsushima, M., Mitsuoka, K., Murata, K., Hirai, T. & Fujiyoshi, Y. (1997). *Nature (London)*, **389**, 206–211.

Kitagawa, T. & Ogura, T. (1997). *Prog. Inorg. Chem.* **45**, 431–476.

Koepke, J., Hu, X., Muenke, C., Schulten, K. & Michel, H. (1996). *Structure*, **4**, 581–597.

Krauss, N., Schubert, W., Klukas, O., Fromme, P., Tobias, H. & Saenger, W. (1996). *Nature Struct. Biol.* **3**, 965–973.

Kuhlbrandt, W., Wang, D. N. & Fujiyoshi, Y. (1994). *Nature (London)*, **367**, 614–621.

Luzzati, V. (1952). *Acta Cryst.* **5**, 802–810.

McDermott, G., Prince, S. M., Freer, A. A., Hawthornthwaite-Lawless, A. M., Papiz, M. Z., Cogdell, R. J. & Isaacs, N. W. (1995). *Nature (London)*, **374**, 517–521.

Malmström, B. G. (1990). *Chem. Rev.* **90**, 1247–1260.

Michel, H. (1983). *Trends Biochem. Sci.* **8**, 56–59.

Michel, H. & Deisenhofer, J. (1987). *Chem. Scr.* **27**B, 173–180.

Ogura, T., Takahashi, S., Shinzawa-Itoh, K. & Yoshikawa, S. (1991). *Bull. Chem. Soc. Jpn*, **64**, 2901–2907.

Ostermeier, C., Harrenga, A., Ermler, U. & Michel, H. (1997). *Proc. Natl Acad. Sci. USA*, **94**, 10547–10553.

Ostermeier, C., Iwata, S., Ludwig, B. & Michel, H. (1995). *Nature Struct. Biol.* **2**, 842–846.

Otwinowski, Z. (1991). *Daresbury Study Weekend Proceedings*, edited by W. Wolf, P. R. Evans & A. G. W. Leslie, pp. 80–86. SERC Daresbury Laboratory, Daresbury, England.

Otwinowski, Z. (1993). *DENZO and SCALEPACK, Data Processing and Scaling Programs*. Yale University, New Haven, CT, USA.

Pebay-Peyroula, E., Rummel, G., Rosenbusch, J. P. & Landau, E. M. (1997). *Science*, **277**, 1676–1681.

Picot, D., Loll, P. J. & Garavito, R. M. (1994). *Nature (London)*, **367**, 243–249.

Ramakrishnan, C. & Ramachandran, G. N. (1965). *Biophys. J.* **5**, 909–933.

Sakabe, N. (1983). *J. Appl. Cryst.* **16**, 542–547.

Shinzawa-Itoh, K., Ueda, H., Yoshikawa, S., Aoyama, H., Yamashita, E. & Tsukihara, T. (1995). *J. Mol. Biol.* **246**, 572–575.

Song, L., Hobaugh, M. R., Shustak, C., Cheley, S., Bayley, H. & Gouaux, J. E. (1996). *Science*, **274**, 1859–1866.

Tomizaki, T., Yamashita, E., Yamaguchi, H., Aoyama, H., Tsukihara, T., Shinzawa-Itoh, K., Nakashima, R., Yaono, R. & Yoshikawa, S. (1998). *Acta Cryst.* D. In the press.

Tsukihara, T., Aoyama, H., Yamashita, E., Tomizaki, T., Yamaguchi, H., Shinzawa-Itoh, K., Nakashima, R., Yaono, R. & Yoshikawa, S. (1995). *Science*, **269**, 1069–1074.

Tsukihara, T., Aoyama, H., Yamashita, E., Tomizaki, T., Yamaguchi, H., Shinzawa-Itoh, K., Nakashima, R., Yaono, R. & Yoshikawa, S. (1996). *Science*, **272**, 1136–1144.

Varotosis, C., Zhang, Y., Appelman, E. H. & Babcock, G. T. (1993). *Proc. Natl Acad. Sci. USA*, **90**, 237–241.

Wallin, E., Tsukihara, T., Yoshikawa, S., von Heijne, G. & Elofsson, A. (1997). *Protein Sci.* **6**, 808–815.

Wang, B. C. (1985). *Methods Enzymol.* **115**, 90–113.

Warburg, O. (1924). *Biochem. Z.* **152**, 479–494.

Wikström, M., Bogachev, A., Finel, M., Morgan, J. E., Puustinen, A., Raitio, M., Verkhovskaya, M. & Verkhovsky, M. I. (1994). *Biochim. Biophys. Acta*, **1187**, 106–111.

Williams, R. J. P. (1995). *Nature (London)*, **376**, 643.

Xia, D., Yu, C., Kim, H., Xia, J., Kachurin, A. M., Zhang, L., Yu, L. & Deisenhofer, J. (1997). *Science*, **277**, 60–66.

Yoshikawa, S., Shinzawa-Itoh, K., Nakashima, R., Yaono, R., Yamashita, E., Inoue, N., Yao, M., Fei, M. J., Peters Libeu, C., Mizushima, T., Yamaguchi, H., Tomizaki, T. & Tsukihara, T. (1998). *Science*, **280**, 1723–1729.

Yoshikawa, S., Tera, T., Takahashi, Y., Tsukihara, T. & Caughey, W. S. (1988). *Proc. Natl Acad. Sci. USA*, **85**, 1354–1358.

Zhang, K. Y. J. & Main, P. (1990). *Acta Cryst.* A**46**, 377–381.

Zhang, Z., Huang, L., Shulmeister, V. M., Chi, Y., Kim, K. K., Hung, L., Croft, A. R., Berry, E. A. & Kim, S. (1998). *Nature (London)*, **392**, 677–684.